International Journal of Scientific Research & Engineering Technology (IJSET)
ISSN: 2356-5608, Vol.3, issue 2
Copyright IPCO-2015-pp.95-101

Simulation and Implementation of a Single Phase Photovoltaic Inveter Based on Voltage Hysteresis PWM Control Strategy

M. Mghezzi Larafi [#1], G. Mohand Kaci [#2], R. Belaidi [#3], M. Hatti [#4], M. Fathi [#5]

[#] *Unité de Développement des Equipements Solaires, UDES / Centre de Développement des Energies Renouvelables, CDER, Bou Ismail, 42415, W. Tipaza, Algérie.*

[1] lm.mghezzi@yahoo.fr

[2] gh_mohandkaci@yahoo.fr

***Abstract*— This work is devoted to the numerical simulation and practical implementation of a photovoltaic single-phase voltage inverter, with pulse width modulation control strategy (PWM) of hysteresis sigma-delta type. We will first present the principle of the adopted control strategy, and the various factors affecting the dynamic performance reported by a hysteresis voltage regulator, which allows carrying out a tracking of the sinusoidal reference control voltage of the studied inverter. On the other hand we will design the output filter of the inverter, whose the size depends directly on the switching frequencies of PWM signal. Finally, we will conduct a comparative study between the simulation results and those of the experimentation.**

***Keywords*— Photovoltaic inverter; Hysteresis PWM control; Regulation; Auto-oscillations; Output filter.**

I. INTRODUCTION

Renewable energies constitute an alternative to fossil fuels which are in depleted, they are called clean energy as they participate in the fight against global warming and CO_2 emissions in the atmosphere, they enter generally in the framework of sustainable development. Solar energy is at the origin of almost all the different forms of renewable energy, which can be exploited in two aspects, photovoltaic or thermal. The application field of photovoltaic energy has become very wide and varied with technological developments; however PV inverters in a broad sense constitute a power conditioning system very essential in various photovoltaic installations. For all these reasons, we propose carrying out the analysis of the various phenomenons, occurring in the hysteresis regulation of sigma-delta type, of the output voltage of a single phase photovoltaic inverter. A practical implantation of the control algorithm will be, thus the comparison of different simulations results with the experimental data.

II. NOMENCLATURE

A, B : state and input matrixes of the continuous state model.
A_d, B_d : state and input matrixes of the sampled state model.
C_f : output filtering capacitor of the inverter.
E : dc input voltage of the inverter.
$f_1(k)$, $\overline{f_1(k)}$, $\overline{f_2(k)}$, $f_2(k)$: connection functions of the dc/ac converter.
f_e, T_e : sampling frequency and sampling period of time.
f_1, ω_1 : fundamental frequency and pulsation.
h: harmonic order.
k: discrete time instant.
K_1, τ_1: gain and time constant of the subtractor-integrator circuit.
L_f et C_f : inductance and capacity of the LC output filter.
m_0 : off-load transformer ratio.
n_A, n_B : order of the square state matrix and the input vector of state model.
r : adjusting coefficient of PWM control.
R_L et L_L: resistance and inductance of load of the inverter.
R_p, L_p : resistance and total leakage inductance referred to the primary side of the transformer.
sign : sign function.
V_{CC}, V_{EE} : bias voltage of the control circuit.
v_H, i_H : output current and voltage of the H bridge
v_{mes} : output voltage of the subtractor-integrator circuit.
v_{ref} : reference voltage of the control
V_{refp} : reference voltage of potentials
Δv, v_0 : input and output voltage of the hysteresis cycle.
v_{0cen}, v_{0amp} : center and magnitude of the hysteresis cycle along of the ordinates axis.
Δv_{cen}, Δv_{amp} : center and a half-width of the hysteresis cycle along the axis of abscissas.
V_h : effective value of the voltage harmonic of h order
V_1 : effective value of the voltage fundamental harmonic component.
THD : rate of harmonic distortion relative to the fundamental.
X, U : state and control vectors of the state model.
Y_1 : Admittance to the fundamental frequency of the nominal load.

III. Principle of the Sigma-Delta Hysteresis PWM Control Strategy

In sigma-delta hysteresis PWM control of a photovoltaic inverter, the comparison of the reference voltage integral with the output voltage integral of the dc/ac converter, allows to generate an error signal, which is injected in the input of a hysteresis regulator, it forces the output voltage of the inverter to evolve inside a voltage band, limited by two switching

International Journal of Scientific Research & Engineering Technology (IJSET)
ISSN: 2356-5608, Vol.3, issue 2
Copyright IPCO-2015-pp.95-101

thresholds upper and lower of the hysteresis cycle, around the integral of the reference voltage, in such manner so that the

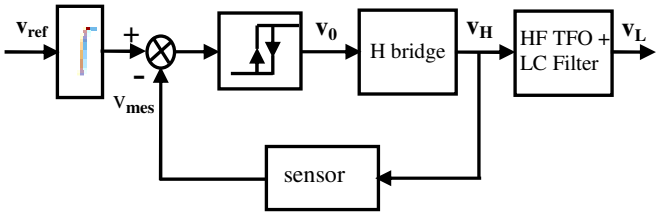

Fig. 1 Block diagram of hysteresis enslavement of the inverter

average value of the H bridge output voltage, be equal to the average value of the reference voltage, during one switching period [1],[2]. The command block diagram (Fig.1) highlights the loop of negative feedback which allows enslaving of the output voltage of the converter to the reference voltage.

The global electric scheme of the inverter is highlighted in Fig. 2. The image of the instantaneous output voltage of the inverter is measured by a voltage sensor which allows splitting and integrating the voltage of the dc/ac converter. If the system to be enslaved is stable and has a step response to monotonous derivative, it is necessary to use a hysteresis element to obtain an operation at a finite frequency, by setting an absolute limit at the differences between the enslaved quantity and the setpoint, so that the regulated variable can follow the temporal evolution of the setpoint within the meaning of the average value. Furthermore, as this type of control is based on the regulation of the rippling of a state variable around a reference quantity, it is necessary that the receptor to be endowed with an inductance, that is ensured by insertion of the output H bridge of the cascade constituted by a high frequency step-up transformer and a filtering capacitor, which act as a power integrator, thus allowing conditioning the signals issued by the converter itself, from the point view of amplitude and waveform, by transforming the voltage pulses delivered by the bridge, into a pure sinusoid, that we seek for supplying the load. Moreover, it will be necessary to

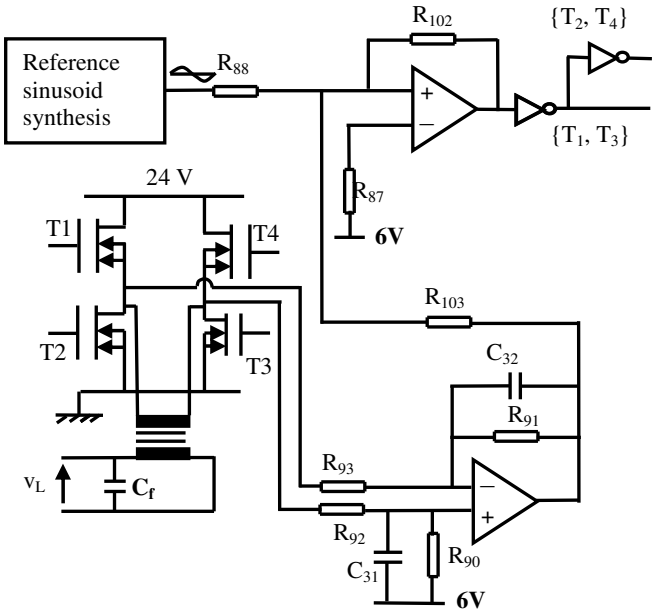

Fig. 2 enslavement diagram of the inverter

provide an effective protection device of the inverter, in case where of an anomaly of operation occurs, it allows to route or block the control signals of the power stage, according on the security state of the inverter, by insuring several functions of protection such as under-voltage, overvoltage, over-temperature, over-current and the short-circuit.

IV. Modelling of the Inverter Controlled by Hysteresis Voltage

We will carry out now a mathematical modelling of a closed loop system, which will allow us to describe the role of the principals parts which compose the inverter, we will study then the dynamic performances reported by this hysteresis corrector.

IV.1. Sensor of Output Voltage of the dc/ac Converter

The available dc voltages are positive, it is thus necessary to carry out a shift of the electrical potentials reference, which allows us to realize a symmetrical control centred around a reference voltage of 6 V, from a bias voltage of 12 V, thanks to a resistive voltage divider whose the impedance is adapted by a buffer stage. The subtractor-integrator circuit indicated in Fig. 3 allows measuring the integral of the output voltage of the dc/ac converter, which represents the image of the output voltage of the inverter, centred on 6 V. The feedback voltage of the regulation loop is taken at the primary output transformer instead of the secondary, this allows avoiding the implementation of a lowering system of voltage from 220 V to 12 V, after having raised it already. This integrator based on the operational amplifier, having the same constant time that the cascade {transformer, output filter}, will give exactly the image of the output sinusoid of the inverter. The continue transfer function, of the subtractor-integrator circuit is given by the expression hereafter :

International Journal of Scientific Research & Engineering Technology (IJSET)
ISSN: 2356-5608, Vol.3, issue 2
Copyright IPCO-2015-pp.95-101

$$H_c(s)=\frac{v_{mes}-v_{refp}}{v_H}=\frac{-K_1}{1+s\,\tau_1} \quad (1)$$

$$\text{with: } K_1=\frac{R_{91}}{R_{93}}, \qquad \tau_1=R_{91}\,C_{32}$$

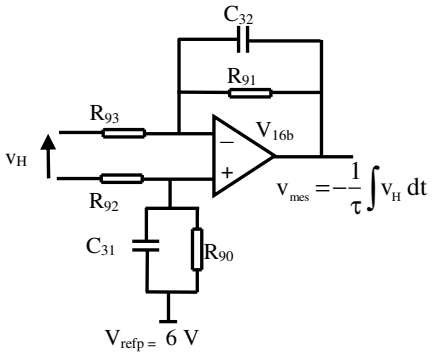

Fig. 3 Subtractor-integrator circuit.

IV.2. Hysteresis Regulator Model

A hysteresis corrector (Fig. 4) compares the image of the output voltage integral of the bridge with the sinusoidal reference voltage integral. The error signal attacks the input of the hysteresis regulator, which generates at its output a pulses train modulated in width, in such manner to perform a nonlinear enslavement of the output voltage of the inverter in the sense of the averages values of each chopping period. The Schmitt trigger which models an on-off element operates according to the hysteresis cycle shown in Fig 5.

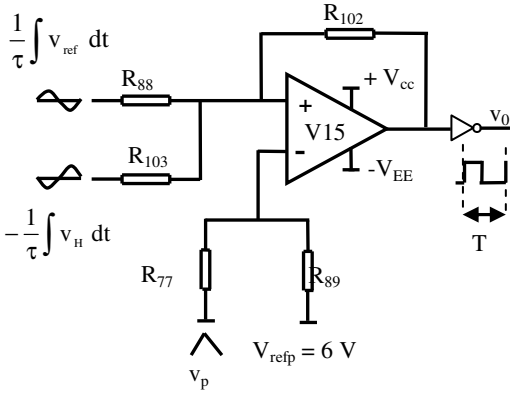

Fig. 4 circuit of voltage hysteresis comparator

The recursive digital model of asymmetric hysteresis cycle is given by the following function :

$$v_0(k+1)=v_{0cen}-v_{0amp}\,\text{sign}(\Delta v(k)-\Delta v_{cen}(k)-\Delta v_{amp} -\text{sign}(v_0(k)-v_{0cen})) \quad (2)$$

The input voltage Δv(k) of the cycle at k instant represents the integral of the difference between the reference signal and the image of the output voltage of the dc/ac converter.

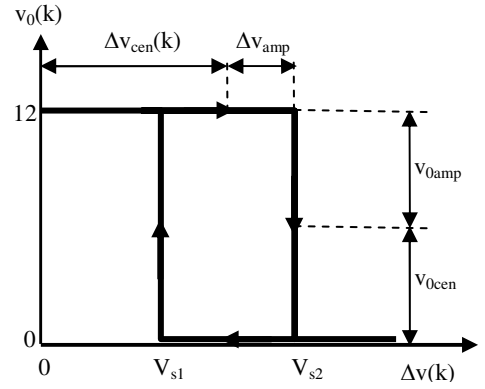

Fig. 5 Diagram of an asymmetric hysteresis cycle modelling a hysteresis regulator.

The switching thresholds voltages of the hysteresis comparator are formulated in the following expressions :

$$V_{S1}=\frac{\left(\frac{R}{R_{102}}+2\right)}{\left(\frac{1}{R_{77}}+\frac{1}{R_{89}}\right)}\left(\frac{v_p}{R_{77}}+\frac{v_{REFP}}{R_{89}}\right)-\left(\frac{R\,V_{cc}}{R_{102}}\right) \quad (3)$$

$$V_{S2}=\frac{\left(\frac{R}{R_{102}}+2\right)}{\left(\frac{1}{R_{77}}+\frac{1}{R_{89}}\right)}\left(\frac{v_p}{R_{77}}+\frac{v_{REFP}}{R_{89}}\right)+\left(\frac{R\,V_{EE}}{R_{102}}\right) \quad (4)$$

With : $R = R_{88} = R_{103}$.

IV.3. Description of the Designed Power Circuit

Figure 6 describes the electrical configuration of the schematic diagram of the power circuit of a photovoltaic single phase voltage inverter full bridge. The interface stage allows on one hand, to realize a galvanic isolation between the control and power circuits, via optocouplers, in order to ensure both the safety of the operator and equipment, and on the other hand, it allows to condition the signals issued from the control circuit of the inverter, thinks to a IR2110 driver by leg of inverter which performs the drive of the power MOSFET transistors, using the bootstrap capacitor technique, allowing to perform a floating mass supply. All input PV inverter disposes of a capacitor of high-capacitance, which has a very important role in maintaining a stable operating point. It has a function of reactive energy accumulator and a filtering function of voltage fluctuations due to the imperfections of the dc voltage source and to the commutations modes. The output transformer provided with a filtering capacity C_f constitute an integral part in the system, considering that the whole acts as a power integrator, which can be represented by a first-order transfer function, indispensable to transform PWM signal into a sinusoidal voltage. We will study the case of the adjunction of a series RL load to the output inverter. The sketch diagram of the designed inverter is visualized in Fig. 7, it is constituted

International Journal of Scientific Research & Engineering Technology (IJSET)
ISSN: 2356-5608, Vol.3, issue 2
Copyright IPCO-2015-pp.95-101

of two electronic boards of control and of power, electrically connected by wiring.

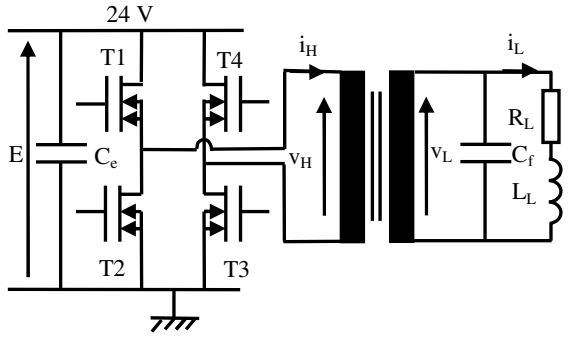

Fig. 6 Power circuit of the single phase photovoltaic inverter on H bridge

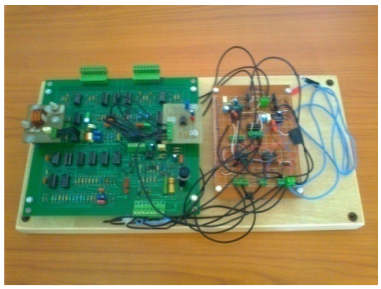

Fig. 7 Photography of the designed photovoltaic inverter

If we respectively associate at the power electronic switches {T1,T2,T3,T4} of the dc/ac converter, the connection functions $\left\{f_1(k), \overline{f_1(k)}, \overline{f_2(k)}, f_2(k)\right\}$ describing their logic states, the model of the dc/ac static converter is given at a discrete time k by the following logical expression :

$$v_H(k) = \frac{E}{2}\left(\left(f_1(k) - \overline{f_1(k)}\right) - \left(f_2(k) - \overline{f_2(k)}\right)\right) \quad (5)$$

For simplification reasons of calculations, it will assume that the model of the transformer gets reduced to the total resistance and the total leakages inductance referred to the primary side, that is to say that we neglect the losses in the magnetization branch of transformer. In such conditions, the continuous linear state model of power system is written in the flowing matrix form:

$$\dot{\mathbf{X}} = A_c \mathbf{X} + B_c \mathbf{U} \quad (6)$$

with :

$$X = \begin{bmatrix} v_{mes} - v_{refp} \\ i_H \\ v_L \\ i_L \end{bmatrix} \qquad U = [v_H]$$

The matrix parameters of the system being:

$$A_c = \begin{bmatrix} \frac{-1}{\tau_1} & 0 & 0 & 0 \\ 0 & \frac{-R_p}{L_p} & \frac{-1}{L_p} & 0 \\ 0 & \frac{1}{C_f} & 0 & \frac{-1}{C_f} \\ 0 & 0 & \frac{1}{L_L} & \frac{-R_L}{L_L} \end{bmatrix} \qquad B_c = \begin{bmatrix} \frac{-K_1}{\tau_1} \\ \frac{1}{L_p} \\ 0 \\ 0 \end{bmatrix}$$

The sampled state model of the regulated linear system, obtained by using a zero-order hold is formulated by:

$$X(k+1) = A_d\, X(k) + B_d\, U(k) \quad (7)$$

The transition from the continuous to the discrete state representation is carried out in the following way:

$$\left[\begin{array}{c|c} A_d & B_d \\ \hline zr(n_B, n_A) & I(n_B, n_B) \end{array}\right] = \exp\left(\left[\begin{array}{c|c} A_c & B_c \\ \hline zr(n_B, n_A) & zr(n_B, n_B) \end{array}\right] T_e\right)$$

With :

$\dim(A_c) = \dim(A_d) = n_A \times n_A$
$\dim(B_c) = \dim(B_d) = n_A \times n_B$
$zr(n_B, n_A)$ et $zr(n_B, n_B)$: zero matrixes respectively of dimension $(n_B \times n_A)$et $(n_B \times n_B)$
$I(n_B, n_B)$: identity matrix of dimension $(n_B \times n_B)$.

The evaluation of the output voltage quality of the inverter is carried out via the calculation of the total harmonic distortion rate compared with a fundamental, that is to say :

$$THD\,(\%) = 100\,\frac{\sqrt{\sum_{h=2}^{+\infty} V_h^2}}{V_1} \quad (8)$$

V. Comparison Between the Simulation Results and the Experimentation

The practical data of the control circuit are:

E = 24 V, V_{cc} = 12 V, V_{EE} = 0 V, V_{refp} = 6 V, v_{0amp} = 6 V, v_{0cen} = 6 V, $\Delta v_{cen}(k)$=0, Δv_{amp} = 0.18 V, r = 0.9, f_e = 800 kHz, f_1 = 50 Hz, K_1 = 0.1471, τ_1 = 0.25 ms, m_0 = 20.

The parameters of the power circuit are:

R_p = 0.015 Ω, $L_f = L_p$ = 8.540 µH, C_f = 4000 µF, R_L = 0.1983 Ω, L_L = 0.3911 mH.

Numerical simulation of the dynamic behaviour of the inverter, debiting on series RL load is carry out in the discrete state space, under the Matlab environment. The experimental and simulated graphs of the integral of the reference voltage, as well as that the error signal representing the difference between the setpoint voltage and the image of the output voltage of the inverter, are visualized respectively in Figs. 8a and 8b, where it manifests voltage peaks due to switching regimes of power MOSFET transistors. The phenomena of

over-band [3] is observed, this is due to the effect of the dynamic of hysteresis regulation in tracking of the variable setpoint, but these over-bands are relatively low for the measured and simulated cases, so basically we can say that the output voltage of the inverter is maintained within the voltage band imposed by the hysteresis regulator. On the other hand, the amplitude of the reference voltage of the control is in a ratio of 2.5/24 in comparison to the dc input voltage of the inverter, while the image of the output voltage is in a more ample ratio of 3.5/24. This avoids the risk of clipping of the output voltage of the inverter during a voltage drop that can reach up to 20 V, beyond what the inverter stops.

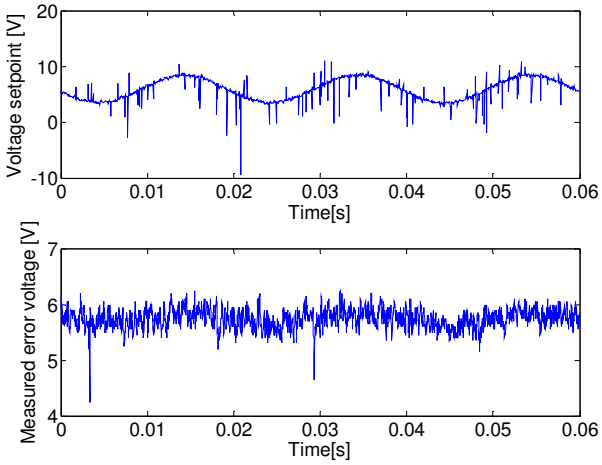

Fig. 8a Measured control signals

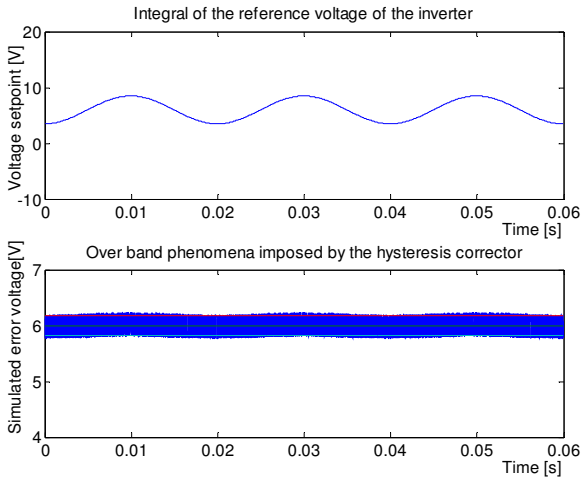

Fig. 8b Simulated control signals

The measured and simulated output voltage of the dc/ac converter in sigma-delta PWM control strategy is characterized by high switching frequencies [4] (Fig. 9a et 9b), it is the result of the non-linear comparison between the two control signals of the inverter. The discrete amplitude spectrums associated to the measured and simulated PWM voltage are practically similar (Fig. 9a and 9b), they are constituted by the lines packets multiples of the fundamental frequency. The rank of the first harmful harmonic having a considerable energy weight, is of the order 173 which corresponds to the frequency of 8.65 kHz, on which is based the design of the LC power output filter, which requires a rigorous harmonic analysis [5], considering that we are constrained to satisfy a compromise, on the one hand between the elimination of the harmful harmonics which are pushed to higher frequencies, thanks to the PWM control law, facilitating thus enormously the filtering operation, and on the other hand the conservation of the amplitude of the fundamental harmonic, while tolerating that a very low allowed attenuation.

Considering that the voltage modulation is carried out at high frequencies, which is in our case of the order of 10 kHz, we can use the leakages inductances of step-up transformer as

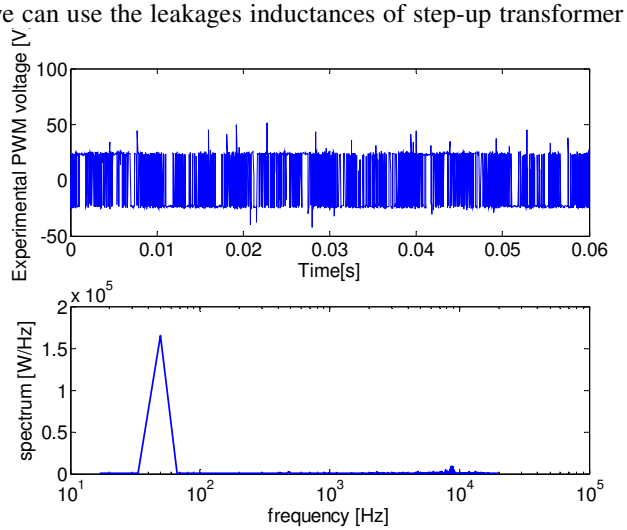

Fig. 9a Measured PWM voltage and its amplitude spectrum

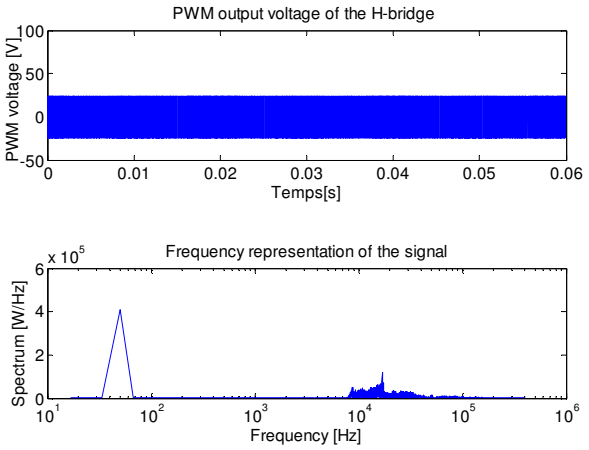

Fig. 9b Simulated PWM Voltage and its amplitude spectrum

an inductor of the LC filter. We have developed a program under the Matlab environment, which allows us to well size an LC filter, using a method described in the first graph in Fig. 10. We denote by U_{s10} and U_{s1} the fundamental harmonic of the output voltage of the filter in off-load and full load. I_{e1} and I_{s1} are the fundamental harmonics of the input and output currents of the filter. U_{enx} and U_{snx} represent the effective values of the first harmful harmonic of nx rank of the input and output voltages of the filter. We use the axes system

($L_f\,\omega_1\,Y_1$) and ($C_f\,\omega_1 / Y_1$), wherein is plotted the networks of curves (C_1), (C_2) and (C_3), respectively of equal ratios (U_{s1}/U_{s10}), (I_{e1}/I_{s1}) and (U_{snx}/U_{enx}). The first ratio allows limiting the voltage drop caused by the filter coil, while the second ratio limits the current absorbed by the filter capacitor. The latest ratio corresponds to the desired minimum attenuation degree for the first harmful harmonic. Considering that the n_x rank of this latter is high, we have imposed tight conditions for the filter design. For a nominal inductive load, these three ratios that allow parameterizing the curves networks are valued as follows:

$$\frac{U_{s1}}{U_{s10}}=0.95 \qquad \frac{I_{e1}}{I_{s1}}=1.1 \qquad \frac{U_{snx}}{U_{enx}}=0.01 \qquad \text{avec } n_x=173$$

The geometrical locus delimited by the three curves defines a curvilinear triangle which constitutes the filter design domain [1]. We ordinarily choose the L_f and C_f filter parameters that correspond to M point of the (C_3) curve, in order to ensure minimal attenuation of harmful harmonics. In our case, the abscissa of the M point is selected so as to coincide the filter inductance with the totals leakages inductance referred to the primary side of the transformer. The results of the design are:

$L_f\,\omega_1\,Y_1 = 0.0115$, $L_f = L_p = 8.540\ \mu H$, $C_f = 4000\ \mu F$.

The gain Bode diagram of LC Lowpass filter is shown in the second graph in Fig. 10. We have a good frequency range, which allows achieving an easy down of the filter. It is clear that the resonant frequency of the filter is sufficiently remote

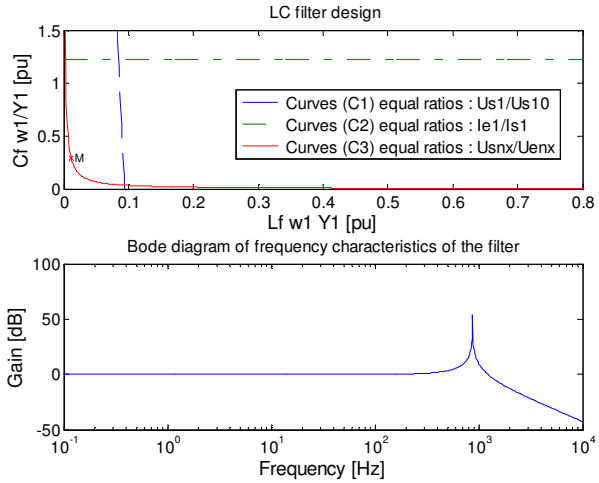

Fig. 10 Design of LC output filter of the inverter

from the fundamental harmonic and the first harmful harmonic, this ensures a good stability of the system.

Figure 11 shows the filtered dynamic temporal responses of the output voltage and current of the inverter, referred to the primary side of the transformer, during a brusque interlocking of the inverter on a RL series load. As the load is of a passive nature, it manifests a very short transient regime, the established regime is quickly reached after small fluctuations, They have a purely sinusoidal waveform. The harmonic distortion rate THD of the output voltage is evaluated at 0.6 %, this shows the good dynamic performances reported by the sigma-delta hysteresis control.

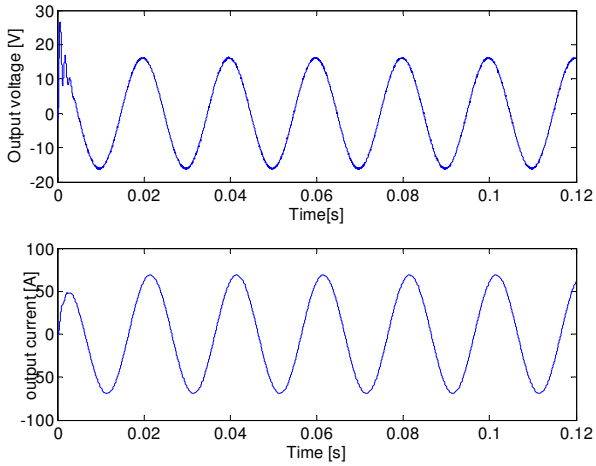

Fig. 11 Dynamic temporal responses of the output voltage and current of the inverter

VI. CONCLUSIONS

The dynamic performances reported by the hysteresis regulation, depend directly on the constant time of the subtractor-integrator circuit, which has considerable influence on the phenomena of over-band of the output voltage inverter. This integration constant should be chosen judiciously, in order to impose a minimum frequency of self-oscillations of the output voltage of the inverter, which is inversely proportional to the hysteresis range, it also depends on the adjusting coefficient of PWM control, which must not exceed a maximum so that the minimum switching frequency be sufficiently high compared to the frequency of the reference signal, which avoids any risk of dropping out of the control. The choice of the sampling period that have a direct report with the regulation quality, must be based on the dynamic of system, and the frequency content of PWM signal, so as to avoid on the one hand the spectral aliasing phenomena, and the other hand the excessive redundancy of the information. In addition, in high frequency PWM control, the simulation shows that the effects of the LC filter on the fundamental harmonic of the output voltage and current of the inverter are very insignificant, considering that the template of the filter is shaped such that the resonance frequency of the filter to be sufficiently remote from the fundamental harmonic and the first harmful harmonic. The results of simulation and experimentation are globally concordant.

REFERENCES

[1] Guy. Séguier, Ed., *Les Convertisseurs de l'Electronique de Puissance: Commande et Comportement Dynamique*. Technique & Documentation, 1998, vol. 5.

[2] Richard Schreier, Gabor C. Temes, *Understanding Delta-Sigma Data Converters,* Ed. IEEE Press, A JOHN WILEY& SONS, INC., PUBLICATION, USA, 2005.

[3] Mohamed Wissem Naouar, "Commande numérique à base de composants FPGA d'une machine synchrone", Doctorat thesis, ENIT Tunis, Tunisia, Dec. 2007.

[4] G. Luckjiff, I. Dobson and D. Divan, "Interpolative Sigma Delta Modulators for High Frequency", *IEEE Power Electronic Applications*, vol. 1, pp. 444–449, 1995.

[5] G. Luckjiff, I. Dobson and D. Divan, "Spectra of Delta-Sigma Modulated Inverters: An Analytical Treatment", *IEEE TRANSACTIONS ON POWER ELECTRONICS*, vol. *I.* NO. 4, pp. 644–654, Oct. 1992.